Journal of Solid State Chemistry **157,** 274–282 (2001)
doi:10.1006/jssc.2000.9050, available online at http://www.idealibrary.com on IDEAL®

Dispersion of NiO Supported on γ-Al_2O_3 and TiO_2/γ-Al_2O_3 Supports

Jun Wang, Lin Dong,[1] Yuhai Hu, Guishan Zheng, Zheng Hu, and Yi Chen

Institute of Mesoscopic Solid State Chemistry, Department of Chemistry, Nanjing University, Nanjing 210093, China

Received July 17, 2000; in revised form November 14, 2000; accepted December 8, 2000; published online February 19, 2001

Laser Raman spectroscopy (LRS), X-ray diffraction (XRD), X-ray photoelectron spectroscopy (XPS), ultraviolet and diffuse reflectance spectroscopy (UV-DRS), and temperature-programmed reduction (TPR) are used to characterize a series of TiO_2/γ-Al_2O_3, NiO/γ-Al_2O_3, and NiO/TiO_2/γ-Al_2O_3 samples. For TiO_2/γ-Al_2O_3 samples, LRS results indicate that the dispersion capacity of titania on γ-Al_2O_3 is about 0.62 mmol 100 m^{-2} γ-Al_2O_3, which is slightly higher than the theoretical value (0.56 mmol 100 m^{-2} γ-Al_2O_3) calculated by the consideration of the incorporation model (Y. Chen and L. F. Zhang, *Catal. Lett.* 12, 51 (1992)). At low TiO_2 loading, $\leq$ 0.62 mmol 100 m^{-2}-γ-Al_2O_3, only highly dispersed titania species are found on the surface, possibly due to the incorporation of the dispersed Ti^{4+} ions into the surface vacancies of γ-Al_2O_3. Increasing the loading amount of titania leads to the formation of crystalline TiO_2 besides the surface-dispersed titania species. The results show that the state of titania is related to its loading on γ-alumina. The results of XRD and UV-DRS show that the dispersion capacity of NiO on titania-modified γ-Al_2O_3 is lower than that of NiO on γ-Al_2O_3, which is probably caused by the decrease of the useable surface vacancies on γ-Al_2O_3 due to the incorporation of the Ti^{4+} ions. TPR results of NiO/γ-Al_2O_3 and NiO/TiO_2/γ-Al_2O_3 samples reveal that the reduction behaviors of NiO dispersed on γ-Al_2O_3 and on titania-modified γ-Al_2O_3 are apparently different. This result emphasizes that the surface structure of the support is important to the properties of the dispersed metal oxide species. The coordination environments of the dispersed titania and nickel oxide species are discussed on the basis of the incorporation model proposed previously. © 2001 Academic Press

Key Words: **dispersion capacity; incorporation model; NiO; TiO_2; γ-Al_2O_3.**

INTRODUCTION

Supported metal oxides have been extensively studied owing to their well-known applications in a variety of industrially important reactions, e.g., ranging from hydrodesulfurization, cracking, polymerization, and partial oxidation of hydrocarbons to selective reduction of nitrogen oxides. Many studies have shown that the nature of the carrier can have dramatic influences on the chemical properties and activities of supported metal oxide catalysts (1–7). Knowledge of the local structure of the catalyst surface and insight into the factors that determine the surface structure play an important role in further development and optimization of supported metal oxide heterogeneous catalytic systems. Characterization of the properties of the supported metal oxide, however, is complicated since several different structures as well as chemical states might coexist in the support metal oxide system. For example, it has been argued that on γ-alumina molybdenum oxide might exist as (1) a monolayer of isolated tetrahedrally coordinated units, (2) a monolayer of octahedrally coordinated and/or polymeric units, (3) surface species consisting of bi- and trilayer structures of molybdenum oxide, or (4) bulk phase crystallites (6). In addition, the formation of nonstoichiometric (two-dimensional) surface compounds through the interaction of metal oxide and support has also been suggested (7). As mentioned by Massoth and Chianelli *et al.* (6, 8), the commonly used techniques in characterizing these systems might cause some confusion. It is not surprising to see that, despite considerable efforts being devoted to this aspect, different explanations on the structure of dispersed oxide species and on the interaction between them and the support can often be found in the literature (6–13).

To fully understand the nature of the surface structure of a supported metal oxide, useful characterization techniques, which can provide detailed information about the molecular structure of the surface metal oxide, must be capable of discriminating those different surface metal oxide species. To date, the characterization techniques that can provide such detailed molecular information, in some systems, are laser Raman spectroscopy (LRS), extended X-ray absorption fine structure (EXAFS), X-ray absorption near-edge spectroscopy (XANES), X-ray photoelectron spectroscopy (XPS), ultraviolet and diffuse reflectance spectroscopy (UV-DRS), etc. Recent work has shown that comparative studies by these techniques can potentially provide valuable information about the character of surface species on supported catalysts. Each of these methods has its own

[1]To whom correspondence should be addressed. E-mail: chem718@nju.edu.cn. Fax: 86-25-3317761.

0022-4596/01 $35.00

specialty as well as limitation, and applying them in compensatory ways has been very helpful and popular.

Titania has attracted much interest as a support material for metals or metal oxides due to its ability to modify the catalytic properties of the supported phase (14, 15). However, some problems related to using TiO_2 as a support have not been solved: (1) high surface area titania ($> 100\ m^2\ g^{-1}$) is in general difficult to obtain; (2) titania with a reasonably large surface area of metastable anatase modification which, upon heating above 750 K, transforms into the denser rutile structure, and this phase transformation is associated with a significant surface area loss. As the substitute materials, TiO_2 supported on various high-surface-area carriers, γ-Al_2O_3 and SiO_2, etc., have been reported (16, 17). Hercules and co-workers have employed the surface spectroscopic techniques, e.g., LRS and XPS, to investigate the chemical state and dispersion of titania supported on γ-alumina as well as the effects of titania on the chemical state and dispersion of a Co/γ-Al_2O_3 catalyst (18). They found that titania was well dispersed on the surface of γ-Al_2O_3, but the different values of dispersion capacity determined by XRD and LRS have not been discussed in their work. In addition, the exact identity of the structure of the dispersed titania is still open for discussion (17–19).

The chemical state and dispersion of nickel oxide supported on γ-alumina have been well established for the past decades according to its wide uses in industrial catalysis (6, 12, 20–22). In the present work, interest has mainly been focused on the study of the dispersion of NiO on γ-alumina and on titania-modified γ-alumina; the different properties shown in NiO/γ-Al_2O_3 and NiO/TiO_2-γ-Al_2O_3 have been compared and discussed by considering the change of γ-alumina surface. With the comparison of the dispersion capacity of the nickel oxide on γ-alumina and on titania-modified γ-alumina, the nature of titania species on the surface of γ-alumina could be deduced. All the results strongly support the suggestion that the surface structure of the support plays an important role in the dispersion and has great influences on the properties of the dispersed oxide species.

EXPERIMENTAL

Instrument. Laser Raman spectra were recorded on a Bruker RFS-100 Fourier transform spectrometer with an InGaAs detector cooled by liquid nitrogen. Raman excitation at 1064 nm was provided by a Nd:YAG laser. The laser power measured at the powder sample (~ 30 mg) was 100 mW, and spectra were accumulated for 50 scans at 4-cm^{-1} resolution in backscattering geometry. The amount of TiO_2 (anatase) present on the TiO_2/γ-Al_2O_3 samples was estimated by comparison of the band intensities for titania-modified γ-alumina samples with those from the mechanical mixtures of TiO_2 (anatase) and γ-alumina, as reported in detail elsewhere (18).

XRD patterns were obtained with a Shimadzu XD-3A diffraction meter employing Ni-filtered Cu$K\alpha$ radiation (0.15418 nm). The X-ray tube was operated at 35 kV and 20 mA. The amount of bulk NiO was determined by XRD quantitative analysis as reported in detail elsewhere using α-alumina powder as a reference (13).

XPS results were recorded with a V.G. Escalab MK II system equipped with a hemispherical electron energy analyzer. The spectrometer was operated at 15 kV and 20 mA, and an aluminum anode (Al$K\alpha = 1486.6$ eV) was used. The C_{1s} signal (285 eV) was taken as the reference to calculate the binding energies (BE).

UV-DR spectra were recorded in the range of 500–800 nm by a Shimadzu UV-240 spectrophotometer with a $BaSO_4$ sample as a reference.

Temperature-programmed reduction (TPR) was carried out in a quartz U-tube reactor, and a 50-mg sample was used for each measurement. Prior to the reduction, the sample was pretreated in a N_2 stream at 373 K for 1 h and then cooled to room temperature. After that, the H_2–N_2 mixture (5% H_2 by volume) was switched on and the temperature was increased linearly at a rate of 10 K min^{-1}. The consumption of H_2 in the reactant stream was detected by a thermal conductivity cell.

Catalyst preparation. γ-Al_2O_3 support, obtained from Fushun Petrochemical Institute in China, was calcined at 923 K for 4 h before it was used for sample preparation and was found to have a BET surface area of 198 $m^2\ g^{-1}$ and pore volume of 0.52 ml g^{-1}.

Titania-modified γ-alumina supports with TiO_2 loadings from 0.07 to 1.66 mmol 100 m^{-2} γ-Al_2O_3 were prepared by nonaqueous impregnation of γ-Al_2O_3 with solutions of titanium(IV) isopropoxide, Ti(O-iPr)$_4$ (Acros Chemical Co.), dissolved in 2-propanol (Shanghai Chemical Plant China). An appropriate amount of Ti(O-iPr)$_4$ was dissolved in 2-propanol, and the total solution volume was equal to approximately twice the pore volume of the support. The samples with the TiO_2 loadings greater than 0.55 mmol 100 m^{-2} γ-Al_2O_3 were prepared by double impregnation of the γ-alumina using one-half the requisite amount of Ti(O-iPr)$_4$ each time. Following the impregnation, the γ-alumina was placed in moist air at room temperature for 2 h to facilitate hydrolysis of Ti(O-iPr)$_4$, and then the Ti(O-iPr)$_4$-modified γ-alumina was dried under ambient conditions for 48 h, followed by further drying in air at 393 K for 4 h. The modified supports were then calcined in the air at 873 K for 6 h. The nitrogen BET surface areas of the titania-modified γ-alumina supports were approximately $20 \pm 5\ m^2\ g^{-1}$ less than that of unmodified γ-alumina. The decrease in the surface area observed in this study for titania-modified γ-alumina was basically consistent with results reported by others (18, 23). The BET surface area of titania-modified γ-alumina with a TiO_2 loading of 0.27 mmol 100 m^{-2}

γ-Al_2O_3 was 180 $m^2 g^{-1}$, which was used as the support for the preparation of $NiO/TiO_2/\gamma$-Al_2O_3 samples in this study.

The NiO/γ-Al_2O_3 and $NiO/TiO_2/\gamma$-Al_2O_3 samples were prepared by impregnating γ-alumina and titania-modified γ-alumina with an aqueous solution containing the required amount of nickel nitrate hexahydrate (A.R.), respectively. Excess water was removed by evaporation at 360 K with stirring. Then, samples were dried at 373 K and calcined at 773 K for 4 h, respectively.

RESULTS AND DISCUSSION

I. Characterization of TiO_2/γ-Al_2O_3 and $NiO/TiO_2/\gamma$-Al_2O_3 Samples

Dispersion of titania on γ-alumina. Figure 1 shows the laser Raman spectra (ranging from 100 to 750 cm^{-1}) of TiO_2/γ-Al_2O_3 samples with different TiO_2 loadings. For a comparison, the LRS spectrum of a mechanical mixture of TiO_2 (anatase) and γ-Al_2O_3 (with TiO_2 loading around 0.13 mmol 100 m^{-2} γ-Al_2O_3) has been recorded, as shown in Fig. 1d. There is no evident Raman signal observed for the TiO_2/γ-Al_2O_3 sample with a TiO_2 loading of 0.55 mmol 100 m^{-2} γ-Al_2O_3, as shown in Fig. 1a, which is in agreement with that reported by Hercules and co-workers (24). The Raman spectra of the TiO_2/γ-Al_2O_3 with TiO_2 loadings of 0.66 and 1.32 mmol 100 m^{-2} γ-Al_2O_3, as shown in Figs. 1b and 1c, present the bands at 144, 401, 516, 641 cm^{-1}, which are the characteristic bands of anatase (25). The intensities of the corresponding bands increase with increasing TiO_2 loadings. The amount of TiO_2 (anatase) formed in the TiO_2/γ-Al_2O_3 samples is estimated by a comparison of the band intensities for the titania-modified γ-alumina samples with those from the mechanical mixtures of TiO_2 (anatase) and γ-alumina, and the corresponding data are listed in Table 1. It can be seen that, for the sample with TiO_2 loading 0.66 mmol 100 m^{-2} γ-Al_2O_3, about 0.04 mmol 100 m^{-2} crystalline TiO_2 is present as anatase. It could be suggested that the dispersion capacity of TiO_2 on γ-alumina is around 0.62 mmol 100 m^{-2} γ-Al_2O_3. This result is in basic accordance with the previous report (18), which showed that the presence of TiO_2 (anatase) was observed in the TiO_2/γ-Al_2O_3 sample with TiO_2 loadings higher than 0.60 mmol 100 m^{-2} γ-Al_2O_3.

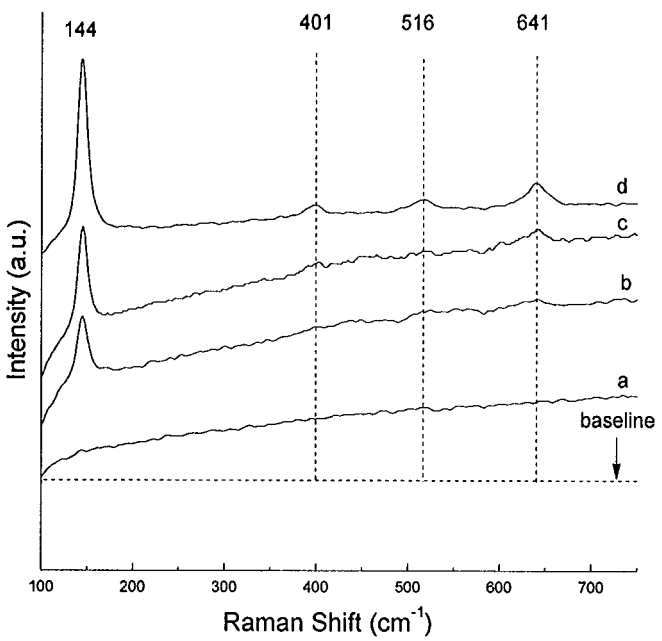

FIG. 1. Raman spectra of TiO_2/γ-Al_2O_3 samples with various TiO_2 loadings (mmol 100 m^{-2} γ-Al_2O_3): (a) 0.55; (b) 0.66; (c) 1.32; (d) a mechanical mixture of TiO_2 (anatase) and γ-Al_2O_3 (0.13 mmol 100 m^{-2} γ-Al_2O_3).

TABLE 1
The Amount of Crystalline TiO_2 on γ-Al_2O_3 Estimated by Laser Raman Spectroscopy

TiO_2 loadings (mmol 100 m^{-2} γ-Al_2O_3)	0.17	0.27	0.33	0.66	1.32
TiO_2 present as anatase (mmol 100 m^{-2} γ-Al_2O_3)	0	0	0	0.04	0.07

Accordingly, at TiO_2 loadings less than 0.62 mmol 100 m^{-2} γ-Al_2O_3, TiO_2 is highly dispersed on γ-alumina; while TiO_2 loadings are beyond 0.62 mmol 100 m^{-2} γ-Al_2O_3, the crystalline TiO_2 (anatase) is formed.

Dispersion of NiO on γ-Al_2O_3 and titania-modified γ-Al_2O_3. As shown in Raman results, there are only surface-dispersed titania species formed in titania-modified γ-Al_2O_3 samples with the titania loading amount of 0.27 mmol 100 m^{-2} γ-Al_2O_3, which is used as the support for the preparation of the $NiO/TiO_2/\gamma$-Al_2O_3 samples. Figure 2 shows the XRD patterns of a series of $NiO/TiO_2/\gamma$-Al_2O_3 samples with different NiO loadings, and the results of γ-alumina, titania-modified γ-alumina, and crystalline NiO, patterns (a), (b), and (i), are also presented for the comparison. For samples with low NiO loadings, i.e., 0.2, 0.4, 0.8, and 1.2 mmol 100 m^{-2} TiO_2/γ-Al_2O_3, no characteristic peaks of crystalline NiO can be observed, as shown in patterns (c), (d), (e), and (f). For the sample with the NiO loading of 1.6 mmol 100 m^{-2} TiO_2/γ-Al_2O_3, pattern (g), characteristic peaks of crystalline NiO (typically with $2\theta = 37.3°$, 43.4°, 63.0°) are observed, and the peak intensity increases with the NiO loadings as shown by a comparison of pattern (h) with pattern (g). The results indicate that nickel oxide exists as highly dispersed surface species in low NiO loading samples; crystalline NiO is also formed in samples with high NiO loadings.

Figure 3 shows the relationship of the amount of the crystalline NiO versus total nickel oxide content in a series of $NiO/TiO_2/\gamma$-Al_2O_3 samples measured by XRD

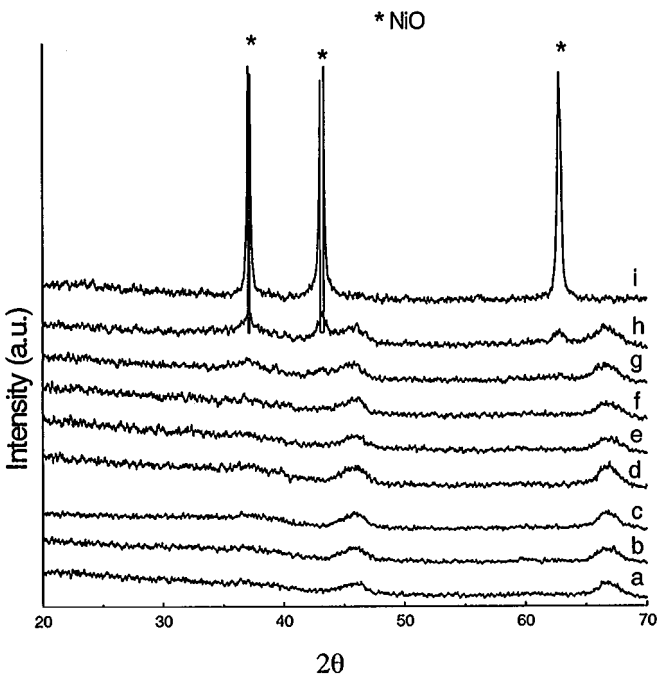

FIG. 2. XRD patterns for the samples (mmol 100 m^{-2} support): (a) γ-Al_2O_3; (b) $TiO_2(0.27)/\gamma$-Al_2O_3; (c) $NiO(0.2)/TiO_2/\gamma$-Al_2O_3; (d) $NiO(0.4)/TiO_2/\gamma$-Al_2O_3; (e) $NiO(0.8)/TiO_2/\gamma$-Al_2O_3; (f) $NiO(1.2)/TiO_2/\gamma$-Al_2O_3; (g) $NiO(1.6)/TiO_2/\gamma$-Al_2O_3; (h) $NiO(2.0)/TiO_2/\gamma$-Al_2O_3; (i) NiO.

quantitative analysis as described elsewhere (13). One can see that there is no crystalline NiO in samples with low NiO loadings, and the straight line representing the formation of crystalline NiO does not go through the origin but gives an intercept on the abscissa at a value referred to as the dispersion capacity, i.e., 1.1 mmol NiO 100 m^{-2} γ-Al_2O_3. Obviously, the dispersion capacity of a metal oxide is a critical value; at values lower than it the metal oxide might become highly dispersed on the support without the formation of its crystalline phase. The above results indicate that the dispersion capacity of nickel oxide on titania-modified γ-alumina is about 1.1 mmol NiO 100 m^{-2} TiO_2/γ-Al_2O_3. Interestingly, the present value seems to be lower than that reported previously for the dispersion capacity of nickel oxide on γ-alumina (about 1.5 mmol 100 m^{-2} γ-Al_2O_3) (26).

UV-DRS results at the band ranging from 500 to 800 nm recorded for the samples with different NiO loadings are shown in Fig. 4. The spectrum of the crystalline NiO is also recorded as a reference, as shown in profile (e). The profile shows that the band at about 725 nm is attributed to the absorption of the crystalline NiO. For the NiO/γ-Al_2O_3 samples, only one band at about 630 nm is observed, as shown in profile (b), which has been attributed to the absorption of surface-dispersed nickel oxide species in the tetrahedral coordination environment (27). For the titania-modified sample, $NiO/TiO_2/\gamma$-Al_2O_3, the absorption profile changes greatly by comparing (c) and (d) with (b). In profiles (c) and (d), new bands at about 725 nm are observed, and the peak intensity increases with the NiO loadings, which should be corresponding to the absorption of formed

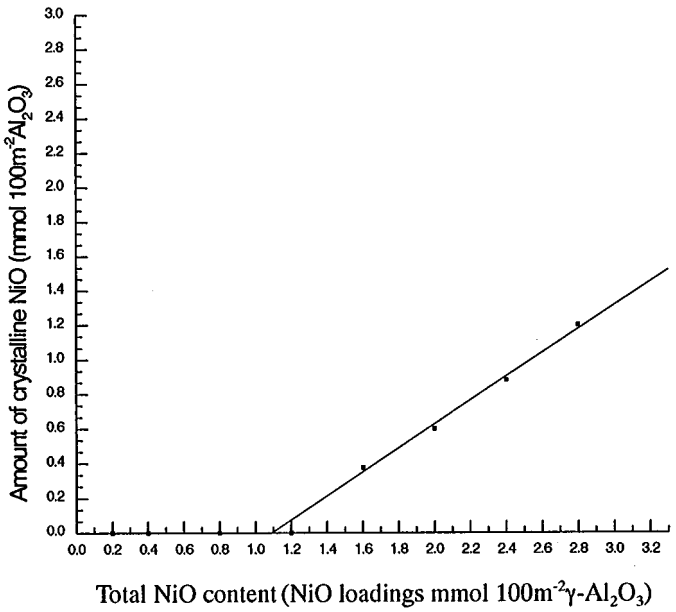

FIG. 3. Amount of crystalline NiO measured by XRD quantitative analysis versus nickel oxide content in $NiO/TiO_2/\gamma$-Al_2O_3 samples.

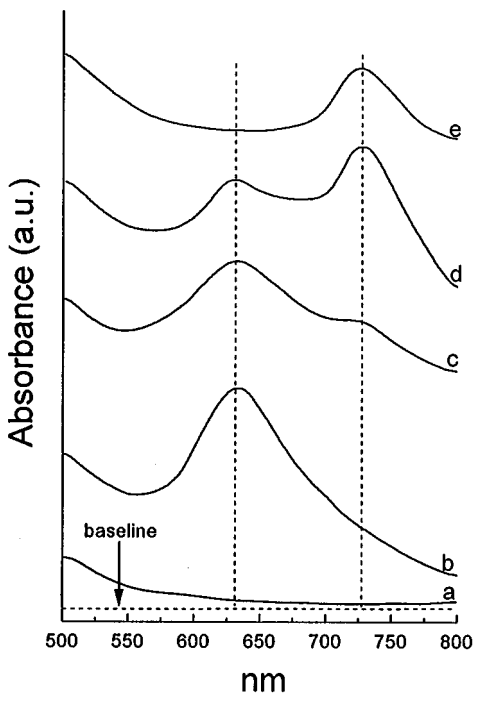

FIG. 4. UV-DR spectra of various samples (mmol 100 m^{-2} support): (a) $TiO_2(0.27)/\gamma$-Al_2O_3; (b) $NiO(1.2)/\gamma$-Al_2O_3; (c) $NiO(1.2)/TiO_2/\gamma$-Al_2O_3; (d) $NiO(2.0)/TiO_2/\gamma$-Al_2O_3; (e) a mechanical mixture of NiO and γ-Al_2O_3 (0.75 mmol 100 m^{-2} γ-Al_2O_3).

crystalline NiO. This result suggests that the nickel oxide species are mainly dispersed on the surface of γ-alumina support and the addition of the titania induces a decreased dispersion capacity for the nickel oxide species on titania-modified γ-alumina.

XPS characterization is used to trace the valence of the relevant elements in the samples. Ni_{2p} and Ti_{2p} spectra are shown in Figs. 5 and 6, respectively, and the BE data are listed in Table 2. The binding energy of $Ni_{2p_{3/2}}$ for nickel oxide species is about 856 eV, which is characteristic of Ni^{2+} (20, 28); all the BE values of $Ti_{2p_{3/2}}$ are about 459 eV, which means that the valences of titania species also stay in 4 + (29, 30). It could be concluded that both nickel oxides species and titania species maintain stable valence on the surface of the γ-alumina.

II. The Reduction Behaviors of NiO/γ-Al_2O_3 and $NiO/TiO_2/\gamma$-Al_2O_3 Samples

TPR results are shown in Fig. 7. For the TiO_2/γ-Al_2O_3 sample, no evident H_2 consumption can be observed, as shown in profile (a), which means that the surface titania species and γ-Al_2O_3 support cannot be evidently reduced at temperatures lower than 1020 K. Profile (b) shows the reduction of the NiO/γ-Al_2O_3 sample with a NiO loading of 1.2 mmol 100 m^{-2} γ-Al_2O_3. Two peaks at 800 and 960 K are observed, which could be presumably ascribed to the reduction of the two different coordinated surface-dispersed nickel oxide species, i.e., octahedral (800 K) and tetrahedral (960 K) site nickel (20, 21). The reduction peaks of titania-modified $NiO/TiO_2/\gamma$-Al_2O_3 samples with different NiO loadings have basic similar profiles, except that there is another peak centered at about 652 K, whose intensity increases with NiO loadings, as shown in profiles (c), (d), and (e). By comparison with profile (f) for the reduction of a mechanical mixture of NiO and γ-Al_2O_3, it seems to suggest that the peak at about 652 K could be corresponding to the reduction of the crystalline NiO formed in the samples. It is worth noting that the reduction peak at 800 K vanishes for the titania-modified $NiO/TiO_2/\gamma$-Al_2O_3 samples as shown in profiles (c), (d), and (e), which is probably due to the absence (or extremely low amount) of octahedrally coordinated surface nickel oxide species in these samples. This result implies that, for the catalyst design, predominant coordinated surface-active species could be obtained by premodification of the surface of the support.

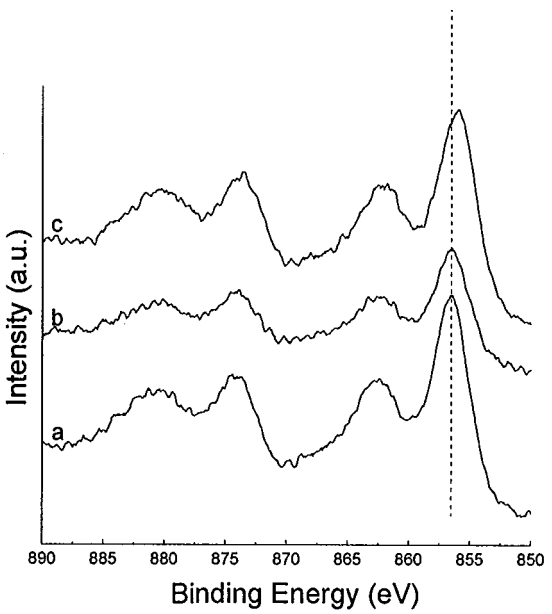

FIG. 5. XPS spectra of Ni_{2p} for various samples (mmol 100 m^{-2} support): (a) $NiO(1.2)/\gamma$-Al_2O_3; (b) $NiO(1.2)/TiO_2/\gamma$-Al_2O_3; (c) $NiO(2.0)/TiO_2/\gamma$-Al_2O_3.

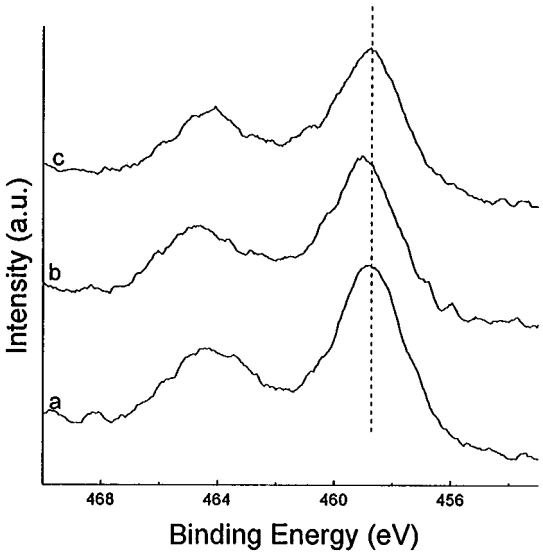

FIG. 6. XPS spectra of Ti_{2p} for various samples (mmol 100 m^{-2} support): (a) $TiO_2(0.27)/\gamma$-Al_2O_3; (b) $NiO(1.2)/TiO_2/\gamma$-Al_2O_3; (c) $NiO(2.0)/TiO_2/\gamma$-Al_2O_3.

TABLE 2
Binding Energies of Various Samples

NiO loadings[a] (mmol 100 m^{-2} γ-Al_2O_3)	Binding energies (eV)	
	$Ni_{2p_{3/2}}$	$Ti_{2p_{3/2}}$
TiO_2/γ-Al_2O_3		458.8
$NiO(1.2)/\gamma$-Al_2O_3	856.5	
$NiO(1.2)/TiO_2/\gamma$-Al_2O_3	856.5	459.0
$NiO(2.0)/TiO_2/\gamma$-Al_2O_3	856.0	458.8

[a] TiO_2 loadings in all the smaples are 0.27 mmol 100 m^{-2} γ-Al_2O_3.

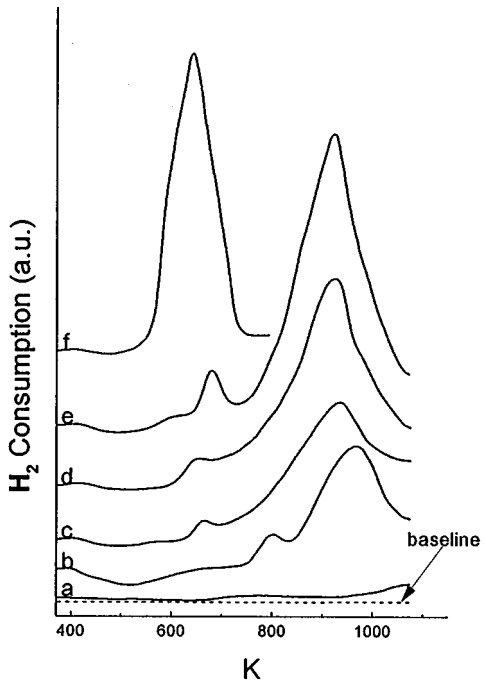

FIG. 7. TPR profiles of various samples (mmol 100 m^{-2} support): (a) $TiO_2(0.27)/\gamma$-Al_2O_3; (b) $NiO(1.2)/\gamma$-Al_2O_3; (c) $NiO(1.2)/TiO_2/\gamma$-Al_2O_3; (d) $NiO(1.6)/TiO_2/\gamma$-Al_2O_3; (e) $NiO(2.0)/TiO_2/\gamma$-Al_2O_3; (f) a mechanical mixture of NiO and γ-Al_2O_3 (0.75 mmol 100 $m^{-2}\gamma$-Al_2O_3).

III. Possible Structures of the Dispersed Surface Nickel Oxide and Titania on γ-Al_2O_3

The properties of the NiO/γ-Al_2O_3 system have been extensively investigated and the state of the dispersed nickel oxide has been proposed (22, 26, 31). Ni^{2+} ions preferentially incorporated into the tetrahedral surface vacancies at low NiO loadings, and both the tetrahedral and octahedral nickel oxide species were present at the high NiO loadings, which led to a dispersion capacity of about 1.5 mmol 100 m^{-2} γ-Al_2O_3 on the surface of γ-Al_2O_3 (26, 31, 32). Thus, as an attempt, the dispersion of nickel oxide was used as a "titration" in studying the dispersion capacity and chemical state of titania dispersed on the surface of γ-alumina, e.g., by comparing the dispersion capacity of the nickel oxide on titania-modified γ-Al_2O_3 with that of NiO on γ-Al_2O_3, and the state of titania species on the surface of γ-Al_2O_3 could be deduced with the consideration of the incorporation model.

As reported previously, two kinds of surface vacant sites, e.g., octahedral and tetrahedral sites, were on the preferentially exposed (110) plane of γ-Al_2O_3 (26, 33). And γ-alumina can be assumed to consist of particles formed by one-dimensional stacking of C- and D-layers. The exposure possibilities of these two layers are equal, as suggested by others (34). Based on the consideration of the incorporation model proposed previously (26, 32), the surface structures of the dispersed titania and nickel oxide species could be proposed. For a TiO_2/γ-Al_2O_3 sample, the dispersed titania could be tentatively described as the incorporation of a Ti^{4+} ion into the surface octahedral vacancy, and then two oxygen anions associated with the cation will stay at the top of the occupied site forming capping oxygen, for the sake of charge compensation, as shown in Fig. 8. Accordingly, the dispersed titania species on the surface of the γ-alumina support can be schematized, as shown in Fig. 9. For a NiO/γ-Al_2O_3 sample, when a Ni^{2+} ion incorporates in the tetrahedral site of γ-alumina, a four-coordination dispersed nickel oxide species is formed, and the structure of the nickel oxide species is shown in Fig. 10. While if only one Ni^{2+} ion incorporates in the octahedral site of γ-alumina without other incorporated Ni^{2+} ions around it, a five-coordinated nickel oxide species will be formed.

Based on the consideration of the incorporation model, at most two Ti^{4+} ions can be implanted in a unit mesh (the area of each unit mesh is 0.443 nm^2 based on the radius of the O^{2-} ion being 0.14 nm) of the D-layer, and one Ti^{4+} ion can be incorporated in a unit mesh of the C-layer. After all the usable sites are occupied, the capping oxygen anions form an epitaxial layer on the top of the γ-alumina surface, as shown in Fig. 9. Along these lines, the dispersion capacity of TiO_2 on γ-Al_2O_3 can be estimated to be 0.56 mmol 100 m^{-2} γ-Al_2O_3, and the dispersion capacity of NiO supported on the titania-modified γ-alumina with a titania loading amount of 0.27 mmol TiO_2 100 m^{-2} γ-Al_2O_3 can be estimated to be about 1.0 mmol 100 m^{-2} γ-Al_2O_3, which

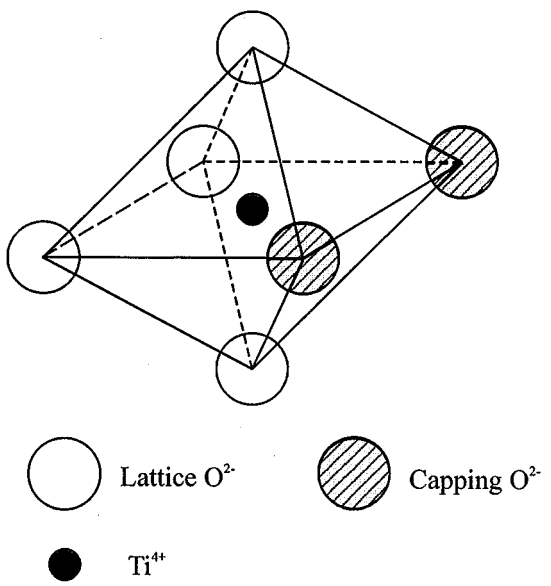

FIG. 8. Tentative model of the surface-dispersed titania species formed on the (110) plane of γ-Al_2O_3 support.

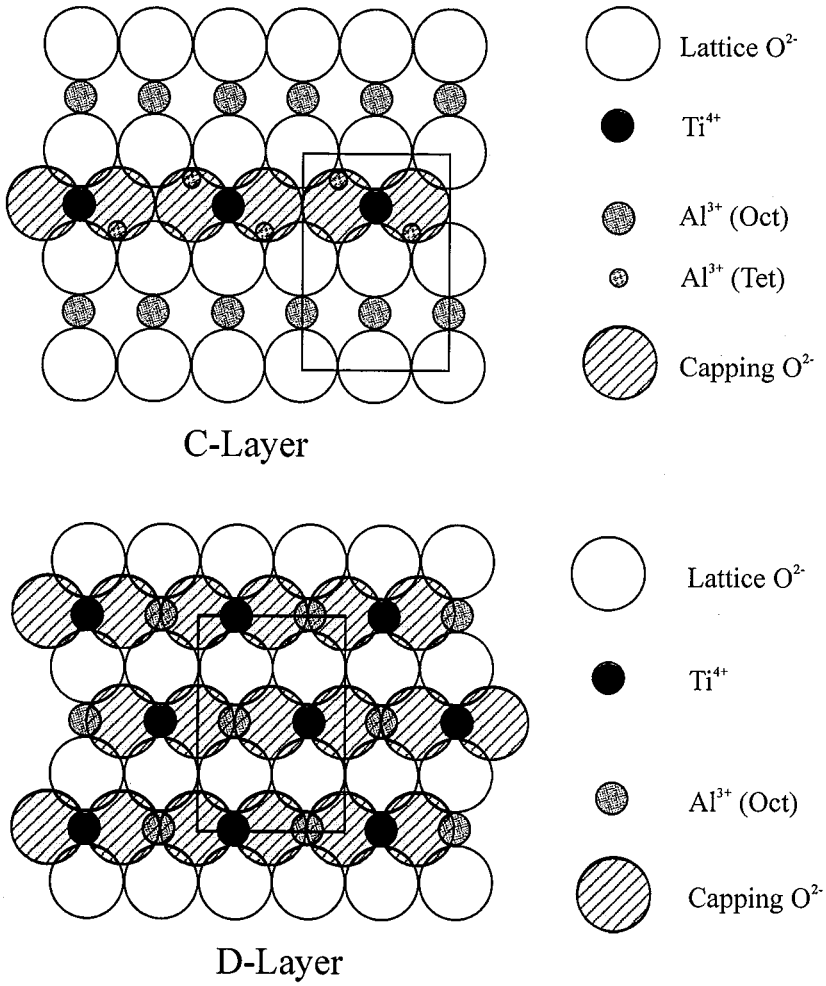

FIG. 9. The schematic diagram for the incorporated Ti^{4+} ions in the surface vacant sites of the (110) plane of γ-Al_2O_3.

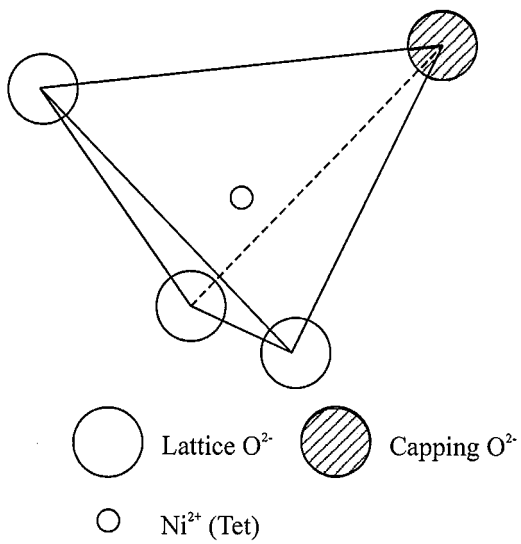

FIG. 10. Tentative model of the surface-dispersed nickel oxide species formed on the (110) plane of γ-Al_2O_3 support with a Ni^{2+} ion incorporating in a tetrahedral vacant site.

is lower than the dispersion capacity of nickel oxide on γ-alumina, e.g., 1.5 mmol 100 m^{-2}. The dispersion of nickel oxide species on the titania-modified γ-alumina surface with low titania loading is schematically shown in Fig. 11. Consequently, all the calculations, as shown in Table 3, are basically consistent with the LRS and XRD results.

CONCLUSION

LRS results have shown that a highly dispersed titania species on the surface of γ-alumina is formed and the dispersion capacity of TiO_2 is about 0.62 mmol 100 m^{-2} γ-Al_2O_3. XRD results of the $NiO/TiO_2/\gamma$-Al_2O_3 samples have shown that the dispersion capacity of NiO on the titania-modified γ-alumina (with a titania loading of 0.27 mmol 100 m^{-2} γ-Al_2O_3) is about 1.1 mmol 100 m^{-2} γ-Al_2O_3, which is lower than that of NiO on an unmodified γ-alumina support.

TPR and UV-DRS results of NiO/γ-Al_2O_3 and $NiO/TiO_2/\gamma$-Al_2O_3 samples indicate that the dispersion

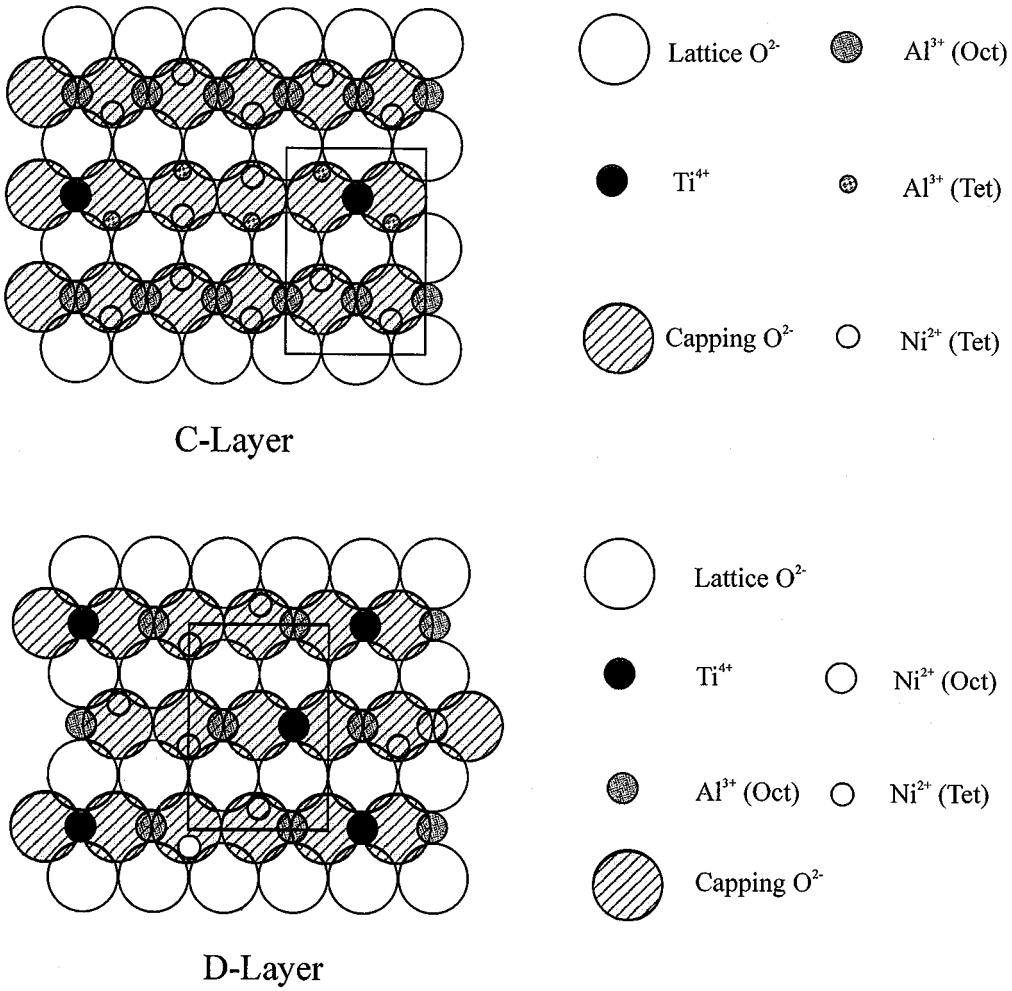

FIG. 11. The schematic diagram for the incorporated Ti^{4+} ions and Ni^{2+} ions in the surface vacant sites of the (110) plane of γ-Al_2O_3.

behaviors and properties of the metal oxide species are strongly related to the surface structure of the support.

Based on the consideration of the incorporation model, it seems to suggest that the surface-dispersed titania on γ-Al_2O_3 should be in the state of the symmetric six-coordinated Ti^{4+} species by the incorporation of Ti^{4+} ions into the surface octahedral vacancies on the preferentially exposed (110) plane of γ-Al_2O_3. Consequently, the dispersion capacity of NiO on titania-modified γ-alumina is decreased due to the occupation of the surface vacancies by Ti^{4+} ions.

TABLE 3
Dispersion Capacities of TiO_2 on γ-Al_2O_3 and NiO on Titania-Modified γ-Al_2O_3

Systems	Experimental value (mmol 100 m^{-2} support)	Estimated value (mmol 100 m^{-2} support)
TiO_2/γ-Al_2O_3	~ 0.62 (0.60)[a]	0.56
$NiO/TiO_2/\gamma$-Al_2O_3	~ 1.1	1.0

[a] The experimental value of TiO_2 on γ-Al_2O_3 is reported by Hercules (18).

ACKNOWLEDGMENT

We acknowledge support from Special Grants for Doctoral Studies (98028434), the Ministry of Education, China.

REFERENCES

1. C. H. Bartholomew and R. C. Reuel, *J. Catal.* **85,** 78 (1984).
2. C. H. Bartholomew and G. K. Vance, *J. Catal.* **91,** 78 (1985).
3. K. Y. S. Ng and E. Gulari, *J. Catal.* **95,** 33 (1985).
4. K. Y. S. Ng and E. Gulari, *J. Catal.* **92,** 340 (1985).
5. M. A. Vannice, C. C. Twu, and S. A. Moon, *J. Catal.* **79,** 70 (1983).
6. F. E. Massoth, *Adv. Catal.* **27,** 265 (1978).
7. G. T. Pott and W. H. J. Stork, *in* "Preparation of Catalysts" (B. Delmon, P. A. Jacobs, G. Poncelet, Eds.), p. 537. Elsevier, Amsterdam, 1976.

8. R. R. Chianelli, M. Daage, and M. J. Ledoux, *Adv. Catal.* **40,** 177 (1994).
9. H. P. Boehm and H. Knözinger, *in* "Analysis, Science and Technology" (J. R. Anderson and M. Boudart, Eds.), Vol. 4, p. 39. Springer-Verlag, West Berlin, 1983.
10. H. Knözinger and E. Taglauer, *in* "Catalysis (A Specialist Periodical Report)" (J. J. Spivey and S. K. Agarwal, Eds.), Vol. 10, p. 1. The Royal Society of Chemistry, London, 1993.
11. Yu. I. Yermakov, B. N. Kuznetsov, and V. A. Zakarov, *in* "Analysis by Supported Complexes." Elsevier, Armsterdam, 1981.
12. B. Delmon and M. Houalla, *in* "Preparation of Catalysts II" (B. Delmon, P. Grange, P. A. Jacobs, and G. Poncelet, Eds.), p. 447. Elsvier, Amsterdam, 1979.
13. Y. Xie and Y. Tang, *Adv. Catal.* **37,** 1 (1990).
14. G. C. Bond and R. Burch, *in* "Catalysis (Specialist Periodical Report)," Vol. 6, p. 27. The Chemical Society, London, 1983.
15. I. Nova, L. Lietti, L. Casagrande, Dall'Acqua, E. Giamello, and P. Forzatti, *Appl. Catal. B* **17,** 245 (1998).
16. L. L. Murrell and D. J. C. Yates, *Stud. Surf. Sci. Catal.* **7,** 1470 (1981).
17. K. Foger and J. R. Anderson, *Appl. Catal.* **23,** 139 (1986).
18. M. A. Stranick, M. Houalla, and D. M. Hercules, *J. Catal.* **106,** 362 (1987).
19. M. A. Vuurman and I. E. Wachs, *J. Phys. Chem.* **96,** 5008 (1992).
20. M. Wu and D. M. Hercules, *J. Phys. Chem.* **83,** 2003 (1979).
21. L. F. Zhang, J. F. Lin, and Y. Chen, *J. Chem. Soc. Faraday Trans.* **88,** 497 (1992).
22. Y. Zhang, Y. Xie, Y. Zhang, D. Zhang, and Y. Tang, *Sci. China* (*Ser. B*) **8,** 805 (1986).
23. G. B. McVicker and J. J. Ziemiak, *J. Catal.* **95,** 473 (1985).
24. D. S. Zingg, L. E. Makovsky, R. E. Tischer, F. R. Brown, and D. M. Hercules, *J. Phys. Chem.* **84,** 2898 (1980).
25. U. Balachandran and N. G. Eror, *J. Solid State Chem.* **42,** 276 (1982).
26. Y. Chen and L. F. Zhang, *Catal. Lett.* **12,** 51 (1992).
27. M. L. Jacono, M. Schivavello, and A. Cimino, *J. Phys. Chem.* **75,** 1044 (1971).
28. K. S. Kim and N. Winograd, *Surf. Sci.* **43,** 625 (1974).
29. G. B. Raupp and J. A. Dumesic, *J. Phys. Chem.* **89,** 5240 (1985).
30. L. Ramqvist, K. Hamrin, G. Johansson, A. Fahlmann, and C. Nordling, *J. Phys. Chem. Solids* **30,** 1835 (1969).
31. L. W. Bruggraf, D. E. Leyden, R. L. Chin, and D. M. Hercules, *J. Catal.* **78,** 360 (1982).
32. Y. Chen, L. F. Zhang, J. F. Lin, and Y. S. Jin, *in* "Catalytic Science and Technology" (S. Yoshida, N. Takezawa, and T. Ono, Eds.), Vol. 1, p. 291. Kodansha, Tokyo, 1990.
33. J. P. Beaufils and Y. Barbaux, *J. Chim. Phys.* **78,** 347 (1981).
34. G. A. Schuit and B. C. Gates, *AIChE J.* **19,** 417 (1973).